COBEM 2021 26th International Congress of Mechanical Engineering
ABCM Associação Brasileira de Engenharia e Ciências Mecânicas
November 22-26, 2021, Virtual Congress, Brazil

COBEM-2021-1445
THERMO-ECONOMIC ANALYSIS OF LOW-GWP REFRIGERANTS IN CASCADE REFRIGERATION SYSTEM WITH R744

Hugo José Abreu de Souza
Paulo Eduardo Lopes Barbieri
Ralney Nogueira de Faria
Tiago de Freitas Paulino

Centro Federal de Educação Tecnológica de Minas Gerais, CEFET-MG, Av. Amazonas, 7675, Nova Gameleira , Belo Horizonte, Minas Gerais, Brasil.
hugo23abreu@gmail.com
barbieri@cefetmg.br
ralneyfaria@gmail.com
tfpaulinoeng@gmail.com

Abstract. *Cascade refrigeration systems are widely used in commercial refrigeration because of their compactness and their ability to provide two different cooling demands at medium and low temperature with high values of COP compared with single-stage vapor compression cycles. Thus, for low-temperature cycle,* CO_2 *(R744) is commonly used due to its low-cost, environmental advantages and the high working pressures at low temperatures. For the high temperature cycle, R134a (GWP100: 1300) and R404A (GWP100: 3943), as well as its corresponding drop-ins, are the most used solutions due to its feasibility, availability and good performance. Because of environmental problems related to global warming effects, research on alternative refrigerant has attracted interest. Despite the large number of works, there are a limited number of analyses that evaluate thermo-economically the use of low-GWP refrigerants in a cascade high temperature cycle. This paper presents a comparative study with different low-GWP refrigerants alternatives to replace R134a in an R134a/R744 cascade system. It considered R32, R450A, R454C, R513A, R1234yf, R290, R600a and R1270 as options in high temperature cycle. Evaluation and optimization of the thermodynamic and economic performance were conducted by EES (Engineering Equation Solver). From the simulations results is demonstrated that the use of R1270 is the best option for high temperature cycle.*

Keywords: *Cascade refrigeration, Thermo-economic analysis, Low-GWP refrigerants, R744*

1. INTRODUCTION

Energy saving and environment protection has been an important issue all over the world. Supermarkets have massive cooling load and traditionally employ synthetic refrigerants. Thus, they contribute significantly towards direct and indirect global warming (Purohit et al, 2017). Approximately half of the energy consumption in a supermarket is associated with the refrigeration system (Mota-Babiloni et al, 2015) In addition fifteen percent of the electricity consumed worldwide is used for refrigeration and the cold-chain accounts for approximately 1% of CO_2 emission in the world (Tassou et al., 2011).

Since the Montreal (1987) and Kyoto (1997) protocols, many efforts were performed to evaluate replacements of the CFC, HCFC and HFC (Bolaji and Huan, 2013, Sharma et al., 2014, Antunes and Bandarra Filho, 2016, Mota-Babiloni et al, 2017, Panato et al, 2017, Makhnatch et al, 2019, Heredia-Aricapa et al, 2020).

Carbon dioxide has received considerable attention as an alternative to the commonly used synthetic refrigerants in supermarket refrigeration systems, in an effort to develop systems with lower environmental impact (Sharma et al., 2014). Although CO_2 has a high critical pressure (7.38 MPa) and a low critical temperature (30.97 °C), its high operating pressure leads to a high vapor density and thus a high volumetric refrigeration capacity. The volumetric refrigerating capacity of CO_2 (22,545 kJ/m³ at 0 °C) is 3-10 times larger than CFC, HCFC, HFC and HC refrigerants (Kim et al., 2004). In addition, carbon dioxide has no Ozone Depletion Potential (ODP); a Global Warming Potential (GWP) of one; it is nontoxic, nonflammable and inexpensive (Sharma et al., 2014). Carbon dioxide as a refrigerant has been reported to be used in indirect, cascade and trans-critical cycles (Gupta, D.K., Dasgupta, 2014).

A cascade system is comprised of separate high-temperature and low-temperature circuits, coupled through a heat exchanger called the cascade condenser or cascade heat exchanger. The cascade condenser functions as an evaporator for the high temperature circuit and a condenser for the low temperature circuit. Generally, the high-temperature circuit is a single-stage direct expansion system but the low temperature circuit can either be a direct expansion system or a secondary loop system.

In the literature, there are a significant part of studies that investigate the CO_2 cascade configurations (Sharma et al., 2014, Bellos and Tzivanidis, 2019). The majority of the studies investigate systems with CO_2 in the low-temperature circuit and in the high-temperature circuit, usually, natural refrigerants are used with NH_3 (Lee et al, 2006, Bingming et al, 2009, Rezayan et al, 2011, Yilmaz et al. 2018, Gholamian et al, 2018, Dokandari et al. 2018), as well as R290 and R1270 to be also interesting cases. (Bellos and Tzivanidis, 2019).

Cascade systems and secondary loop systems using CO_2 as a refrigerant can be used to reduce the direct impact on the environment due to their lower HFC refrigerant charge (Sharma et al., 2014) and this system seems to be more efficient than the others, especial for the warm climates (Catalán-Gil et al 2018). The use of CO_2 in the low stage solves the problem of the low critical point which leads to the trans-critical operation and also makes the system to operate with lower pressure levels (Bellos and Tzivanidis, 2019).

This paper presents a comparative study with different low-GWP refrigerants alternatives to replace R134a (GWP_{100}: 1300) in an R134a/R744 cascade system. It considered R32 (GWP_{100}: 675), R450A (GWP_{100}: 574), R454C (GWP_{100}: 146), R513A (GWP_{100}: 573), R1234yf (GWP_{100}: 4), R290 (GWP_{100}: 3), R600a (GWP_{100}: 3) and R1270 (GWP_{100}: 3) as options in high temperature cycle. Evaluation and optimization of the thermodynamic (energy and exergy) and economic performance were conducted by EES (Engineering Equation Solver) (Klein, 2020). The major contribution of this paper is to quantify the benefits in energy and economic perspective for the various low-GWP refrigerants in high-temperature circuit of cascade refrigeration system.

2. METHODOLOGY

In this paper a combined CO_2 secondary/cascade refrigeration system proposed by Sharma et al. (2014) was modeled. The schematic diagram of the modeled system is shown in Figure 1.

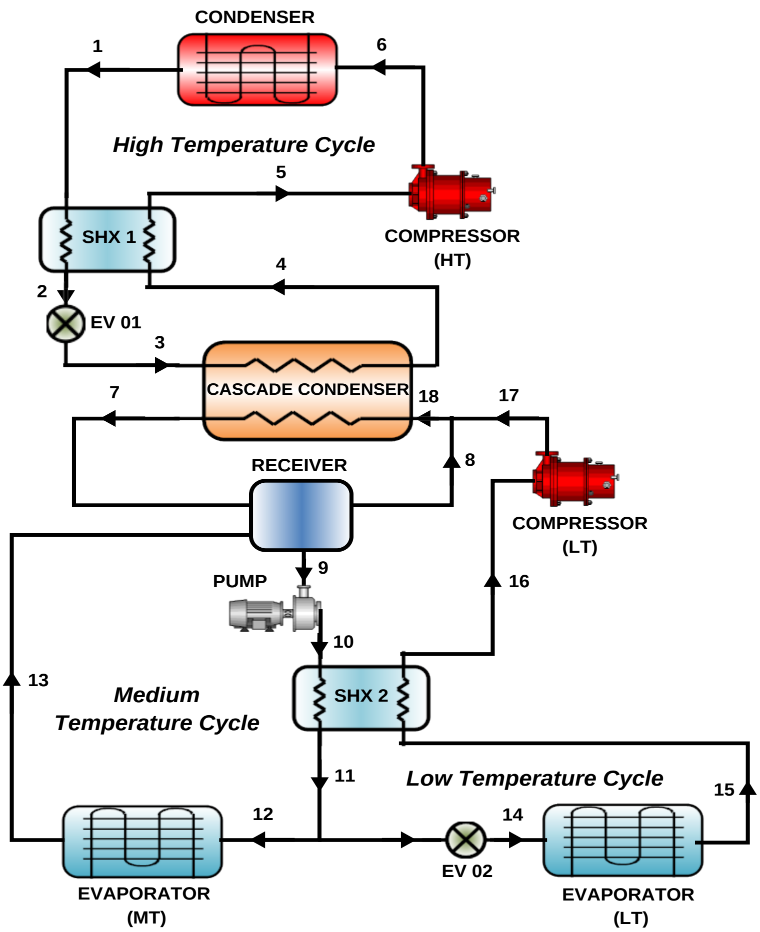

Figure 1. Schematic of combined CO_2 secondary/cascade refrigeration system.

2.1 Thermodynamic Modeling

Thermodynamic modeling includes mass, energy and entropy balance for all components of the cycle along with the reasonable assumption as follows:

1. The system operates under steady state;
2. Only saturated liquid and saturated vapor exit the receiver;
3. The expansion processes were considered isenthalpic;
4. The pressure drop and heat loss/gain in the lines were ignored;
5. The pump isentropic efficiency ($\eta_{s,pump}$) is assumed to be 65%;
6. Work input by the pump is assumed 1% of work input of compressor low-temperature, $\dot{W}_{pump} = 0.01\dot{W}_{comp,LT}$ (Sharma et al. 2014);
7. The kinetic and potential energies are not considered;
8. Evaporator and Condenser Fans are not considered;
9. Saturated refrigerant occurs at the exit of evaporator LT, cascade condenser, condenser.

The following sets of governing equations are applied to all components of cycle while considering it as a control volume.

I. Mass Balance:

$$\sum \dot{m}_{in} = \sum \dot{m}_{out} \tag{1}$$

II. Energy Balance:

$$\dot{Q} + \sum_{in} \dot{m}_{in} h_{in} = \sum_{out} \dot{m}_{out} h_{out} + \dot{W} \tag{2}$$

III. Entropy Generation:

$$\dot{S}_{ger} = \sum_{out} \dot{m}_{out} s_{out} - \sum_{in} \dot{m}_{in} s_{in} - \sum_{k} \frac{\dot{Q}_k}{T_k} \geq 0 \tag{3}$$

IV. Exergy Destruction (Gouy–Stodola equation):

$$\dot{E}x_D = T_o \dot{S}_{ger} \tag{4}$$

where $\dot{m}$ is the mass flow rate, $\dot{Q}$ is the heat transfer, h is the specific enthalpy, $\dot{W}$ is the compressor or pump power, s is the specific entropy, T is the absolute temperature, $\dot{S}_{ger}$ is the entropy generation and $\dot{E}x_D$ is the exergy destruction.

Governing equations used for the thermodynamic modeling of individual components of systems are given in Table 1; wherein the state points are referred to Figure 1.

Table 1. Governing equations for different components of system.

Component	Equations	Component	Equations
Compressor LT	$\dot{W}_{comp,LT} = \dot{m}_{16}\left(h_{17} - h_{16}\right)$ (5) $\dot{E}x_{D,comp,LT} = T_o \dot{m}_{16}\left(s_{17} - s_{16}\right)$ (6) $\eta_{s,comp,LT} = \frac{(h_{17s} - h_{16})}{(h_{17} - h_{16})}$ (7)	Compressor HT	$\dot{W}_{comp,HT} = \dot{m}_5\left(h_6 - h_5\right)$ (8) $\dot{E}x_{D,comp,HT} = T_o \dot{m}_5\left(s_6 - s_5\right)$ (9) $\eta_{s,comp,HT} = \frac{(h_{6S} - h_5)}{(h_6 - h_5)}$ (10)
Pump	$\dot{W}_{pump} = \frac{\left(\dot{m}_9 v_9 \Delta P_{pump}\right)}{\eta_{s,pump}}$ (11) $\dot{E}x_{D,pump} = T_o \dot{m}_9\left(s_{10} - s_9\right)$ (12) $\eta_{s,pump} = \frac{(h_{10s} - h_9)}{(h_{10} - h_9)}$ (13)	Evaporator LT	$\dot{Q}_{evap,LT} = \dot{m}_{14}\left(h_{14} - h_{15}\right)$ (14) $\dot{E}x_{D,evap,LT} = T_o\left(\dot{m}_{14}\left(s_{15} - s_{14}\right) - \frac{\dot{Q}_{evap,LT}}{T_{camara,LT}}\right)$ (15)
Evaporator MT	$\dot{Q}_{evap,MT} = \dot{m}_{12}\left(h_{13} - h_{12}\right)$ (16) $\dot{E}x_{D,evap,MT} = T_o\left(\dot{m}_{12}\left(s_{13} - s_{12}\right) - \frac{\dot{Q}_{evap,MT}}{T_{camara,MT}}\right)$ (17)	Condenser	$\dot{Q}_{cond} = \dot{m}_6\left(h_6 - h_1\right)$ (18) $\dot{E}x_{D,cond} = T_o\left(\dot{m}_6\left(s_1 - s_6\right) + \frac{\dot{Q}_{cond}}{T_{amb}}\right)$ (19)
Expansion Valve 01	$h_2 = h_3$ (20) $\dot{E}x_{D,EV1} = T_o \dot{m}_2\left(s_3 - s_2\right)$ (21)	Expansion Valve 02	$\dot{m}_{11} - \dot{m}_{12} = \dot{m}_{14}$ (22) $h_{11} = h_{14}$ (23) $\dot{E}x_{D,EV2} = T_o \dot{m}_{14}\left(s_{14} - s_{11}\right)$ (24)

SHX 1	SHX 2
$\dot{Q}_{SHX1} = \dot{m}_1 (h_1 - h_2) = \dot{m}_4 (h_5 - h_4)$ (25)	$\dot{Q}_{SHX2} == \dot{m}_{10} (h_{10} - h_{11}) = \dot{m}_{15} (h_{16} - h_{15})$ (28)
$\dot{E}x_{D,SHX1} = T_o (\dot{m}_1 (s_2 - s_1) + \dot{m}_4 (s_5 - s_4))$ (26)	$\dot{E}x_{D,SHX2} = T_o (\dot{m}_{10} (s_{11} - s_{10}) + \dot{m}_{15} (s_{16} - s_{15}))$ (29)
$\varepsilon_{SHX1} = \frac{\dot{m}_1 (h_1 - h_2)}{\dot{m}_4 cp_4 (T_1 - T_4)} = \frac{\dot{m}_4 (h_5 - h_4)}{\dot{m}_4 cp_4 (T_1 - T_4)}$ (27)	$\varepsilon_{SHX2} = \frac{\dot{m}_{10} (h_{10} - h_{11})}{\dot{m}_{15} cp_{15} (T_{10} - T_{15})} = \frac{\dot{m}_{15} (h_{16} - h_{15})}{\dot{m}_{15} cp_{15} (T_{10} - T_{15})}$ (30)
Cascade-Condenser	**Receiver**
$\dot{m}_{18} = \dot{m}_8 + \dot{m}_{17}$ (31)	$\dot{m}_7 + \dot{m}_{13} = \dot{m}_9 + \dot{m}_{18}$ (34)
$\dot{Q}_{CC} = \dot{m}_3 (h_4 - h_3) = \dot{m}_7 (h_{18} - h_7)$ (32)	$\dot{m}_7 h_7 + \dot{m}_{13} h_{13} = \dot{m}_8 h_8 + \dot{m}_9 h_9$ (35)
$\dot{E}x_{D,CC} = T_o (\dot{m}_3 (s_4 - s_3) + \dot{m}_7 (s_7 - s_{18}))$ (33)	$\dot{E}x_{D,REC} = T_o ((\dot{m}_8 s_8 + \dot{m}_9 s_9) - (\dot{m}_7 s_7 + \dot{m}_{13} s_{13}))$ (36)
$COP = \frac{\dot{Q}_{evap,MT} + \dot{Q}_{evap,LT}}{\dot{W}_{comp,LT} + \dot{W}_{comp,HT} + \dot{W}_{pump}}$ (37)	$\dot{E}x_{D,TOTAL} = \sum_{Components} \dot{E}x_D$ (38) $\eta_{II} = 1 - \left(\frac{\dot{E}x_{D,TOTAL}}{\dot{W}_{comp,LT} + \dot{W}_{comp,HT} + \dot{W}_{pump}} \right)$ (39)

In Equations 5 to 39: η_s is the isentropic efficiency, ε is the effectiveness of the heat exchanger, cp is the specific heat, v is the specific volume, COP is the coefficient of performance and η_{II} is the exergetic efficiency.

In Eq. (7), the isentropic efficiency of compressor LT ($\eta_{s.comp,LT}$) depends on the pressure ratio ($rp_{comp,LT}$) and it is given by Jain et al (2015a):

$$\eta_{s,comp,LT} = 0.00476\, rp^2_{comp,LT} - 0.09238\, rp_{comp.LT} + 0.89810 \tag{40}$$

In Eq. (10), the isentropic efficiency of compressor HT ($\eta_{s.comp,HT}$) depends on the pressure ratio ($rp_{comp,HT}$) and it is given by Jain et al (2015a):

$$\eta_{s,comp,HT} = -0.00097\, rp^2_{comp,HT} - 0.01026\, rp_{comp,HT} + 0.83955 \tag{41}$$

2.2 Economic analysis

In the present study, the investment cost (C) of all the heat exchangers, compressor, pump and expansion valve is considered whereas the cost of refrigerant and connecting pipes is neglected. Sanaye and Malekmohammadi (2004) reported that the sum of the costs of other items such as valves, refrigerant, connecting pipes and the structure of the system contributes 0.84% of the total investment cost. In this research, the reference component costs of a particular type and size reported by Rezayan e Behbahaninia (2011), Mosaffa et.al (2016), Jain et.al (2016) and Jain et.al (2015b) are applied for the components of systems are given in Table 2.

The investment cost of the heat exchangers can be expressed as a function of heat transfer area (A) of each aforementioned component, which can be obtained by Eq. (42) (Bejan and Kraus, 2003).

$$\dot{Q} = UA\Delta T_{ml} \tag{42}$$

where A is the heat transfer area of heat exchangers, U is the overall heat transfer coefficient and ΔT_{lm} is the logarithmic mean temperature difference. In the present study the overall heat transfer coefficient (U) is provided by Silva (2019).

Total cost rate (total annual cost, C_{total}) of the overall system is given by Eq. (43), including investment and maintenance cost rate ($C_{inv,main}$), operational cost rate (C_{op}), and penalty cost rate of CO_2 emission (C_{env}).

$$C_{total} = C_{inv,main} + C_{op} + C_{env} \tag{43}$$

Thus, investment and maintenance cost rate of the overall system can be estimated by Eq. (44).

$$C_{inv,main} = (CRF \cdot MF) \sum C_k \tag{44}$$

where C_k is the investment cost of each component (Table 2), *CRF* is capital recovery factor, depends on interest rate (*i*) and system life time (*n*), as described by Eq. (45). Maintenance factor (*MF*) is taken as 1.06 (Jain et al, 2016).

$$CRF = \frac{i\left(1+i\right)^n}{\left(1+i\right)^n - 1} \tag{45}$$

Operational cost (C_{op}) of the cycles is mainly due to the electricity consumed by compressors and pump, as described by Eq. (46).

$$C_{op} = t_{op}\, C_{ele}[\dot{W}_{comp.LT} + \dot{W}_{comp.HT} + \dot{W}_{pump}] \tag{46}$$

where t_{op} is the annual operating hours and C_{ele} is the electricity price.

Due to the increasing environmental concerns and specifically global warming issues, considering the environmental impacts is becoming essential in modeling of the thermal systems. The penalty cost for CO_2 emission (C_{env}) is calculated by Eq. (47) (Aminyavari et al, 2014).

$$C_{env} = m_{CO2} C_{CO2} \tag{47}$$

In Eq. (47), C_{CO2} is the cost of unit carbon dioxide emission. m_{CO2} is the CO_2 emission mass, which can be determined using emission conversion factor is calculated by Eq. (48) (Sanaye and Shirazi, 2013).

$$m_{CO2} = t_{op}\, \lambda [\dot{W}_{comp.LT} + \dot{W}_{comp.HT} + \dot{W}_{pump}] \tag{48}$$

where λ is the emission conversion factor.

Table 2. Investment cost of each component of the system.

Compressor $C_{comp,LT} = \dfrac{573\,\dot{m}_{16}}{0.8996 - \eta_{s,com,LT}}\, rp_{comp,LT}\, ln(rp_{comp,LT})$ (49) $C_{comp,HT} = \dfrac{573\,\dot{m}_{5}}{0.8996 - \eta_{s,comp,HT}}\, rp_{comp,HT}\, ln(rp_{comp,HT})$ (50)	Pump $C_{pump} = 705.48\dot{W}_{pump}^{0.71}\left(1 + \dfrac{0.2}{1-\eta_{s,pump}}\right)$ (51)
Condenser $C_{cond} = 1397 A_{cond}^{0.89}$ (52)	Receiver $C_{REC} = 280.3\left(\dot{m}_7 + \dot{m}_{13}\right)^{0.67}$ (53)
Evaporator $C_{evap,MT} = 1397 A_{evap,MT}^{0.89}$ (54) $C_{evap,LT} = 1397 A_{evap,LT}^{0.89}$ (55)	Cascade-Condenser $C_{CC} = 385.5\ A_{CC}^{0.65}$ (56)
Expansion Valve $C_{EV1} = 114.5\ \dot{m}_1$ (57) $C_{EV2} = 114.5\ \dot{m}_{14}$ (58)	SHX $C_{SHX1} = 516.621\ A_{SHX1} + 268.45$ (59) $C_{SHX2} = 516.621\ A_{SHX2} + 268.45$ (60)

3. METHODOLOGY

3.1 Simulation parameters

The thermo-economic analyses and optimization of the combined CO_2 secondary/cascade refrigeration system are conducted based on the first and the second laws of thermodynamics. The main thermodynamic parameters for the simulation of the desired cycle system are listed in Table 3. The reference state in exergy destruction of this study is expressed as: T_o=T_{amb} and P_o=101.3 *kPa*.

Thermo-economic modeling of the system has been conducted based on simulation code in EES (Engineering Equation Solver). Ambient temperature ranging between 20°C and 40°C (20°C, 25°C, 30°C, 35°C e 40°C) was used to determine the performance of the system and nine fluids were considered R134a, R32, R450A, R454C, R513A, R1234yf, R290, R600a and R1270 as options in high temperature cycle. The condensation temperature of the cascade-condenser heat exchanger was set equal to the evaporation temperature of the evaporator MT.

Table 3. Input data for combined CO_2 secondary/cascade refrigeration system (Sharma et.al, 2014).

Parameter	**Value**
Medium-temperature space[°C]	-5
Low-temperature space [°C]	-30
Medium cooling load [kW]	120
Low cooling load [kW]	65

The overall heat transfer coefficient, U, is an important parameter for calculating the investment cost of heat exchangers. The reference values of overall heat transfer coefficients for all heat exchangers are listed in Table 4.

Table 4 - Reference values of overall heat transfer coefficients (Silva, 2019).

Heat Exchanger	***U [W/m² °C]***
Condenser	98.7
Cascade-condenser	220.5
Evaporator LT	95.6
Evaporator MT	95.6
SHX 1	12665
SHX 2	3595

For the considered combined CO_2 secondary/cascade refrigeration system the parameters for the economic analysis are given in Table 5.

Table 5. Parameters for the economic analysis (Aminyavari et al, 2014).

Parameter	**Value**
Maintenance factor (*MF*)	1.06
Annual operating hours (t_{op}),	7000 h
System life time (*n*)	15 years
Interest rate (*i*)	14%
Electricity price (C_{ele}),	0.06 US$/kWh
Cost of unit carbon dioxide emission (C_{CO2})	90 US$/ ton_{CO2}
Emission conversion factor (λ)	0.11 kg/kWh (MCTIC,2018)

3.2 System optmization

The present optimization process is devoted to investigate and optimize the combined CO_2 secondary/cascade refrigeration system for typical operational conditions for each working fluid. The evaporator temperature difference LT ($\Delta T_{evap,LT}$), evaporator temperature difference MT ($\Delta T_{evap,MT}$), cascade-condenser temperature difference ($\Delta T_{cascade}$), condenser temperature difference (ΔT_{cond}), superheat SHX 1 ($\Delta T_{sup,SHX1}$), superheat SHX 2 ($\Delta T_{sup,SHX2}$) and pump circulation ratio (RC_{pump}) are selected as the continuous decision variables and the examined range are given in Table 6. In this study, the considered objective function is the exergy destruction, Eq. (38) of the whole cascade system which should be minimized. The Direct Optimization Algorithm is used for minimization of exergy destruction.

Table 6. Considered design parameters for system optimization and their corresponding range of variation.

Parameter	**Range of variation**
$\Delta T_{cascade}$, [°C]	3 - 15
ΔT_{cond}, [°C]	5 - 20
$\Delta T_{evap,LT}$, [°C]	5 - 15
$\Delta T_{evap,MT}$ [°C]	5 - 15
$\Delta T_{sup,SHX1}$, [°C]	5 - 15
$\Delta T_{sup2,SHX2}$, [°C]	5 - 15
RC_{pump}	1.25 - 3

4. RESULTS AND DISCUSSION

4.1 Model validation

To validate the model of this work, the data calculated by the current model is compared to those of Sharma et.al, (2014). As shown in Figure 2, data of the present work matches very well to the ones reported by Sharma et.al, (2014), in other words, the largest deviation is 0.0172%.

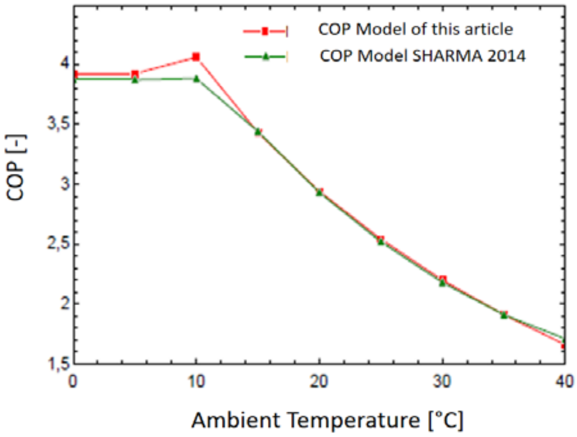

Figure 2. Model validation for different ambient temperatures

4.2 Model results

The optimal differences of temperature, superheat and pump circulation ratio for combined CO_2 secondary/cascade refrigeration system are shown in Table 7. Note that the superheat SHX 1($\Delta T_{sup,SHX1}$) is the same for all fluids evaluated except for the R32.

Table 7. Optimal differences of temperature, superheat and pump circulation ratio for combined CO_2 secondary/cascade refrigeration system.

Refrigerant	$\Delta T_{cascade}$ [°C]	ΔT_{cond} [°C]	$\Delta T_{evap,LT}$ [°C]	$\Delta T_{evap,MT}$ [°C]	$\Delta T_{sup,SHX1}$ [°C]	$\Delta T_{sup,SHX2}$ [°C]	RC_{pump} [-]
R134a	3.02	5.03	5.02	5.02	15.00	5.02	1.84
R32	3.02	5.03	5.02	5.02	5.02	5.02	1.84
R450A	3.02	5.03	5.02	5.02	15.00	5.02	1.84
R454C	3.02	5.03	5.02	5.02	15.00	5.02	1.84
R513A	3.02	5.03	5.02	5.02	15.00	5.02	1.84
R1234yf	3.02	5.03	5.02	5.02	15.00	5.02	1.84
R290	3.02	5.03	5.02	5.02	15.00	5.02	1.84
R600a	3.02	5.03	5.02	5.02	15.00	5.02	1.84
R1270	3.02	5.03	5.02	5.02	15.00	5.02	1.84

The COP and Exergy Destruction of combined CO_2 secondary/cascade refrigeration system and at different ambient temperature is plotted in Figure 3.

It is observed in Figure 3(a) that the COP increases with the reduction of the ambient temperature, Figure 3(b) shown that the exergy destruction rises with the increase of the ambient temperature for all the fluids evaluated. In Figure 3 it is also noted that there is a small variation in the values of COP and Exergy Destruction between the refrigerants evaluated in which R1270 and R600a presented a slightly better behavior.

The volumetric flow rate in the suction of the compressor HT and compressor HT discharge temperature of combined CO_2 secondary/cascade refrigeration system and at different ambient temperature is plotted in Figure 4.

The volumetric flow rate in the suction of the compressor is a parameter that influences the dimensions of the compressor, thus, higher volumetric flow rates are associated with a higher capacity compressor. In Figure 4(a), it is observed that R32 has the lowest volumetric flow rate in the suction and, on the other hand, R600a is the one with the highest volumetric flow rate in the suction. It is also observed that the ambient temperature has little influence on the volumetric flow rate in the compressor suction.

In Figure 4(b), it is observed that R32 has the highest compressor discharge temperature in relation to the other refrigerants evaluated. The compressor discharge temperature is another parameter that must be evaluated in order to avoid premature decomposition of the lubricating oil.

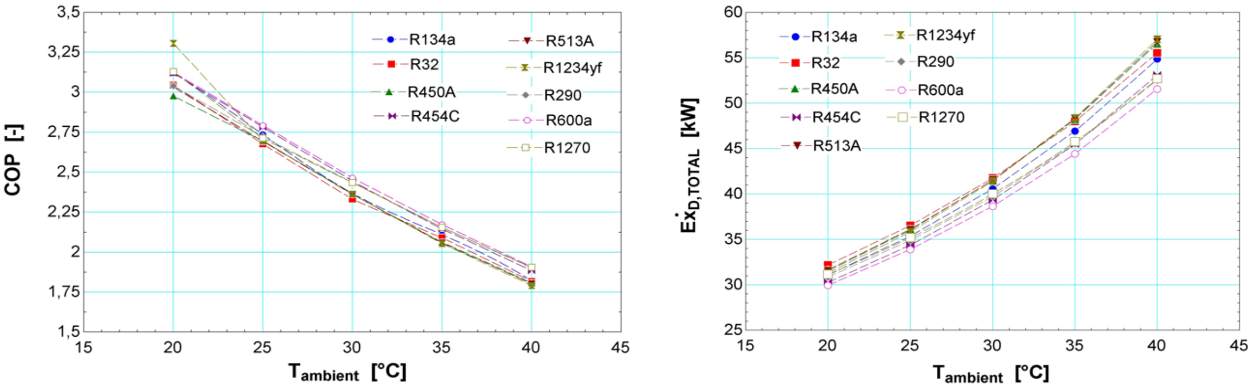

(a) COP (b) Exergy Destruction

Figure 3. Comparison of COP and Exergy Destruction of combined CO_2 secondary/cascade refrigeration system at different ambient temperature.

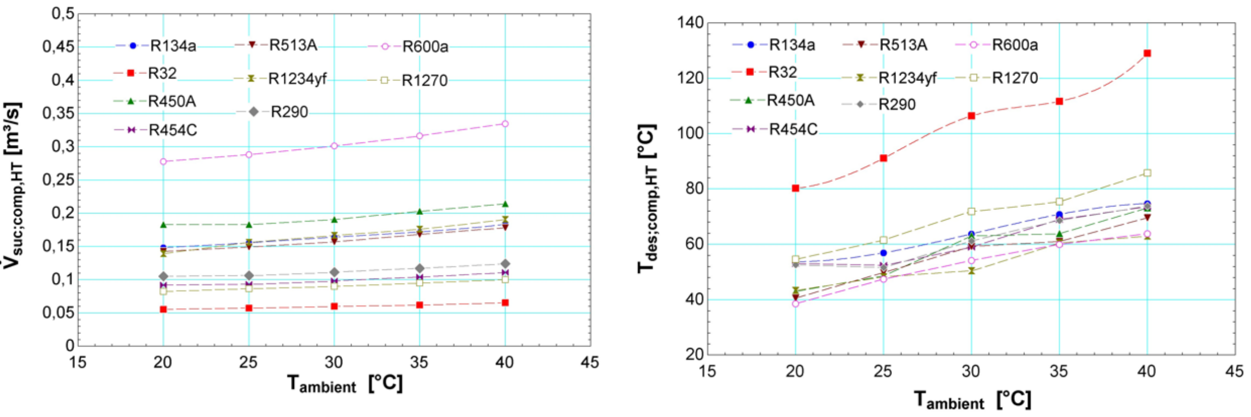

(a) Volumetric flow (b) Discharge temperature

Figure 4. Comparison of volumetric flow rate in the suction of the compressor HT and compressor HT discharge temperature of combined CO_2 secondary/cascade refrigeration system at different ambient temperature.

Considering the results presented in Figure 3(a), it can be observed that, regardless of the refrigerant fluid, the variation in the ambient temperature had a great influence on COP. Thus, in order to assess the behavior of the system in a more critical condition (lower COP), Table 8 presents the results obtained by the thermo-economic model of the system for an ambient temperature of 40°C.

From the analysis of the data in Table 8, it is possible to observe that the refrigerant fluids present similar values for the analyzed parameters. However, it is notable that hydrocarbon fluids (R600a, R290 and R1270) present a performance above the others, allied to a lower total cost. The synthetic fluid that came closest to hydrocarbons was R454C, with practically the same COP. However, it has a total cost about 3% higher.

5. CONCLUSION

Considering the results obtained by the thermo-economic model used to evaluate the use of low-GWP refrigerant fluids in the high temperature cycle in combined CO_2 secondary/cascade refrigeration system, it is concluded that between the fluids evaluated, the hydrocarbon family (R290, R600a and R1270) are the ones that present the best ratio between total cost and performance. Among these fluids, the R1270 presented the lowest total cost, disregarding the costs of installing and maintaining safety systems associated with the use of flammable refrigerants.

Table 8. Results obtained for refrigeration system for an ambient temperature of 40°C.

Parameter	**R134a**	**R32**	**R450A**	**R454C**	**R513A**
COP [-]	1.82	1.81	1.80	1.88	1.80
η_{II} [%]	38.24	38.14	37.94	39.56	37.83
$\dot{E}x_{D,total}[kW]$	54.87	55.55	56.54	53.12	56.78
$\dot{W}_{comp,HT}[kW]$	88.65	88.47	90.00	86.02	90.28
$\dot{W}_{TOTAL}\ [kW]$	101.48	101.73	102.29	98.09	102.57
$\dot{m}_{\mathbf{R744},LT}\ [kg\ /\ s]$	0.247	0.245	0.247	0.247	0.247
$\dot{m}_{\mathbf{R744},MT}\ [kg\ /\ s]$	0.634	0.627	0.894	0.900	0.894
$\dot{m}_{\mathbf{comp}\,HT}\ [kg\ /\ s]$	1.517	0.846	1.610	1.568	1.759
$\dot{V}_{\mathbf{suc},\mathbf{comp}\,HT}\ [m^3\ /\ s]$	0.183	0.065	0.214	0.111	0.178
P_{cond} *[kPa]*	1170	2815	1038	1949	1229
$T_{\mathbf{des},\mathbf{comp}\,HT}\ [°C]$	74.73	129.00	73.14	73.65	69.57
$C_{inv,main}\,[US\$\,/\ yr]$	160,359	154,819	163,238	160,072	163,788
$C_{op}\ [US\$\,/\ yr]$	42672	42785	43014	41248	43134
$C_{env}\ [US\$\,/\ yr]$	7,041	7,060	7,097	6,806	7,117
$C_{TOTAL}\,[US\$\,/\ yr]$	210,144	204,733	213,422	208,198	214,113

Parameter	**R1234yf**	**R290**	**R600a**	**R1270**
COP [-]	1.79	1.90	1.90	1.90
η_{II} [%]	37.59	39.89	40.07	40.00
$\dot{E}x_{D,total}[kW]$	57.04	52.55	51.57	52.69
$\dot{W}_{comp,HT}[kW]$	90.93	85.00	84.77	84.56
$\dot{W}_{TOTAL}\ [kW]$	103.22	97.26	96.84	97.00
$\dot{m}_{\mathbf{R744},LT}\ [kg\ /\ s]$	0.247	0.246	0.247	0.246
$\dot{m}_{\mathbf{R744},MT}\ [kg\ /\ s]$	0.894	0.631	0.900	0.890
$\dot{m}_{\mathbf{comp}\,HT}\ [kg\ /\ s]$	1.950	0.788	0.829	0.751
$\dot{V}_{\mathbf{suc},\mathbf{comp}\,HT}\ [m^3\ /\ s]$	0.190	0.124	0.335	0.100
P_{cond} *[kPa]*	1162	1545	608.7	1859
$T_{\mathbf{des},\mathbf{comp}\,HT}\ [°C]$	62.97	73.85	63.84	85.80
$C_{inv,main}\,[US\$\,/\ yr]$	164,956	155,924	155,730	154,285
$C_{op}\ [US\$\,/\ yr]$	43,404	40,901	40,724	40,792
$C_{env}\ [US\$\,/\ yr]$	7,162	6,749	6,720	6,731
$C_{TOTAL}\,[US\$\,/\ yr]$	215,596	203,643	203,244	201,877

6. REFERENCES

Antunes, A. H. P., Bandarra Filho, E. P., 2016, “Experimental investigation on the performance and global environmental impact of a refrigeration system retrofitted with alternative refrigerants”. *International Journal of Refrigeration*, vol. 70, n° 1, pp. 119-127.

Bejan, A.; Kraus, A. D., 2003, Heat Transfer Handbook. Wiley.

Bellos, E.; Tzivanidis, C., 2019, “A Theoretical Comparative Study of CO_2 Cascade Refrigeration Systems”. *Appl. Sci.*, vol. 9, p.790. https://doi.org/10.3390/app9040790

Bingming, W.; Huagen, W.; Jianfeng, L.; Ziwen, X., 2009, “Experimental investigation on the performance of NH_3/CO_2 cascade refrigeration system with twin-screw compressor”. *International Journal of Refrigeration*, vol. 32, pp.1358–1365.

Bolaji, B.O., Huan, Z., 2013. “Ozone depletion and global warming: case for the use of natural refrigerant – a review”. *Renew.Sustain. Energy* Rev. vol. 18, pp.49–54.

Catalán-Gil, J.; Sánchez, D.; Llopis, R.; Nebot-Andrés, L.; Cabello, R., 2018, “Energy Evaluation of Multiple Stage Commercial Refrigeration Architectures Adapted to F-Gas Regulation”. *Energies*, vol.11, pp.1915.

Dokandari, D.A.; Hagh, A.S.; Mahmoudi, S.M.S., 2014, “Thermodynamic investigation and optimization of novel ejector-expansion CO_2/NH_3 cascade refrigeration cycles (novel CO_2/NH_3 cycle)”. *International Journal of Refrigeration*, vol. 46,pp. 26–36.

Gholamian, E.; Hanafizadeh, P.; Ahmadi, P., 2018, “Advanced exergy analysis of a carbon dioxide ammonia cascade refrigeration system”. *Appl. Therm. Eng*., vol. 137, pp. 689–699.

Gupta, D.K., Dasgupta, M.S., 2014. “Simulation and performance optimization of finned tube gas cooler for trans-critical CO2 refrigeration system in Indian context”. *Int. J. Refrigeration*, vol. 38, pp. 153–167.

Heredia-Aricapa, Y., Belman-Flores. J. M., Mota-Babiloni, A., Serrano-Arellano, J., García-Pabón, J. J., 2020, “Overview of low GWP mixtures for the replacement of HFC refrigerants: R134a, R404A and R410A”, *International Journal of Refrigeration*, vol. 111, pp. 113-123.

Jain, V.; Sachdeva, G; Kachhwaha, S. S., 2015a, “Thermodynamic modeling and parametric study of a low temperature vapor compression-absorption system based on modified Gouy-Stodola equation”, *Energy*, vol. 79, pp. 407-418.

Jain, V.; Sachdeva, G.; Kachhwaha, S. S., 2015b, “Energy, exergy, economic and environmental (4E) analyses based comparative performance study and optimization of vapor compression-absorption integrated refrigeration system”. *Energy*, vol. 91, pp. 816-832. ISSN 0360-5442

Jain V, Sachdeva G, Kachhwaha SS, Patel B., 2016, “Thermo-economic and environmental analyses based multi-objective optimization of vapor compression-absorption cascaded refrigeration system using NSGA-II technique”. *Energy Convers Manage*; vol.113. pp.230–342.

Kim, M.H., Pettersen, J., Bullard, C.W., 2004. “Fundamental process and system design issues in CO_2 vapor compression systems”. *Prog. Energy Combust. Sci*., vol. 30, pp.119-174.

Klein, S.A., 2020, “EES – Engineering Equation Solver”, Version 10.836, F-Chart Software, http://fchartsoftware.com

Lee, T.-S.; Liu, C.-H.; Chen, T.-W., 2006, “Thermodynamic analysis of optimal condensing temperature of cascade-condenser in CO2/NH3 cascade refrigeration systems”. *Int. Journal of Refrigeration*, vol. 29, pp. 1100–1108.

Makhnatch, P., Mota-Babiloni, A., López-Belchí, A., Khodabandeh, R., 2019, “R450A and R513A as lower GWP mixtures for high ambient temperature countries: Experimental comparison with R134a”. *Energy*, vol. 166, pp. 223.

MCTIC – Ministério da Ciência, Tecnologia, Inovações e Comunicações. Fator Médio – Inventários corporativos (tCO2/MWh), 2018. Disponível em: < https://www.mctic.gov.br/mctic/opencms/ciencia/SEPED/clima/textogeral/emissao_corporativos.html>.

Mosaffa,A.H.; Farshi, L.G.; Ferreira, C.A.I.; Rosen, M.A., 2016, “Exergoeconomic and environmental analyses of CO_2/NH_3 cascade refrigeration systems equipped with different types of flash tank intercoolers”. *Energy Conversion and Management*. vol. 117, pp. 442 – 453.

Mota-Babiloni, A., Navarro-Esbrí, J., Barragán-Cervera, A., Molés, F., Peris, B. and Verdú, G, 2015, “Commercial refrigeration e An overview of current status”. *International Journal of Refrigeration*, vol. 57, n° 1, pp. 186-196.

Panato, V. H., Porto, M. P., Bandarra Filho, E. P., 2017, “Experimental performance of an R-22-based refrigeration system for use with R-1270, R-438A, R-404A and R-134a”. *Int. Journal of Refrigeration*, vol. 83, pp. 108-117.

Purohit N., Gupta, D. K., Dasgupta, M. S., 2017, “Energetic and economic analysis of trans-critical CO_2 booster system for refrigeration in warm climatic condition”. *International Journal of Refrigeration*, vol. 80, n° 1, pp. 182-196.

Rezayan, O.; Behbahaninia, A., 2011, “Thermoeconomic optimization and exergy analysis of CO_2/NH_3 cascade refrigeration systems”. *Energy* , vol. 36, n° 1**,** pp. 888–895.

Sanaye S, Malekmohammadi H., 2004, “Thermal and economical optimization of air conditioning units with vapor compression refrigeration system”. *Appl Therm Eng;* vol. 24, n° 13: pp. 1807–1825.

Sanaye S, Shirazi A., 2013, “Four E analysis and multi-objective optimization of an ice thermal energy storage for air conditioning applications”. *Int J Refrig* ,vol.36, n° 3, pp.828–841.

Sharma, V., Fricke, B., Bansal, P., 2014. “Comparative analysis of various CO_2 configurations in supermarket refrigeration systems”. *International Journal of Refrigeration*, vol. 46, pp. 86–99.

Silva, T.,P., 2019, “Simulação termoeconômica de sistemas de refrigeração de ciclo transcrítico e subcrítico utilizando CO_2” (in Portuguese). Master’s Thesis, Graduate Program in Engineering of Energy, Federal Center of Technologic Education of Minas Gerais, Belo Horizonte, Brazil.

Tassou, S.A., Ge, Y.T., Hadawey, A., Marriott, D., 2011. “Energy consumption and conservation in food retailing”. *Appl. Therm.Eng*. vol. 31, pp. 147-156.

Yilmaz, B.; Mancuhan, E.; Erdonmez, N., 2018, “A Parametric Study on a Subcritical CO_2/NH_3 Cascade Refrigeration System for Low Temperature Applications”. *ASME. J. Energy Resour. Technol*., vol. 140, n°9. https://doi.org/10.1115/1.4039976

7. RESPONSIBILITY NOTICE

The authors are the only responsible for the printed material included in this paper.